Tellus (1995), 47A, 383–402
Printed in Belgium – all rights reserved

TELLUS
ISSN 0280-6495

Interaction of a cold front with a sea-breeze front Observations

By B. BRÜMMER[1]*, B. HENNEMUTH[2], A. RHODIN[2] and S. THIEMANN[1], [1]*Meteorologisches Institut der Universität Hamburg*; [2]*Max-Planck-Institut für Meteorologie, Bundesstraße 55, 20146 Hamburg, Germany*

(Manuscript received 11 March 1993; in final form 10 October 1994)

ABSTRACT

On 9 May 1989, during the field experiment FRONTEX, a synoptic-scale cold front was observed which moved from the North Sea to Northern Germany and interacted with a sea-breeze front. The modification of the cold front is documented by satellite images and measurements over the sea, at the coast and further inland. The synoptic-scale front was characterized by weak frontal gradients over the sea. It was aligned approximately parallel to the coast as was approximately the wind ahead of it. While the synoptic-scale front approached the coast during the forenoon hours, a strong temperature contrast developed between sea and land due to solar heating of the land surface. This led to the formation of a sea-breeze front associated with a stronger temperature gradient than the synoptic-scale front. At about noon, when the synoptic-scale front almost reached the coast, the sea-breeze front began to move inland. The onshore wind behind the sea-breeze front and ahead of the synoptic-scale front was so large that the wind field at the synoptic-scale front changed from confluence to difluence. This process was supported by a shallow inversion ahead of the synoptic-scale front which confined the vertical depth of the sea-breeze. The former sea-breeze front overtook the main frontal characteristics, continued its inland propagation and was the only frontal event observed over the land. As a result of the interaction, the synoptic-scale front was significantly intensified in the boundary layer.

1. Introduction

Atmospheric fronts are influenced dynamically and thermodynamically by the underlying surface. Surface friction modifies the cross-frontal circulation and the shape of the frontal surface in the boundary layer (Ball, 1960; Egger, 1988; Dunst and Rhodin, 1990). Different surface heat and moisture fluxes on both sides of the front may act frontogenetically or frontolytically (Kurz, 1982; Koch, 1984). Land and sea surfaces with their differences in roughness, temperature, heat capacity, heat conductivity, moisture and albedo influence the surface layer of the front in different ways.

The frontal temperature contrast in the surface layer is generally weaker over the sea than over land (Rhodin, 1991) due to the nearly constant sea-surface temperature and the reduced frictional convergence. Although vigorous fronts are also observed over the oceans (Bond and Fleagle, 1985; Bond and Shapiro, 1991) the temperature contrast in the lower part of the boundary layer is small. This is confirmed by recent observations of cold fronts over the English Channel during the experiment Fronts '87 (Lagouvardos et al., 1992, their Fig. 3). Over land the low-level temperature contrast at cold fronts can be enhanced by diabatic processes such as prefrontal heating by insolation (Kurz, 1982; Brümmer, 1988). Numerical simulations of cold fronts made by Rhodin (1991) demonstrate that the low-level frontal convergence over land depends on the time of the day and is generally maximum in the afternoon, a consequence of solar radiation.

* Corresponding author.

The preceding considerations suggest that a front will be modified when it moves from sea to land. The thermodynamically induced modification is supposed to increase with increasing temperature difference between sea and land surface. On the other hand strong sea-land temperature contrasts are known to favour the formation of a mesoscale circulation in the coastal area, the sea-land breeze. Mesoscale circulations at the coast can also develop as a consequence of frictional convergence (Bergeron, 1949; Roeloffzen et al., 1986). If the prefrontal temperature and wind conditions are favourable for the generation of such mesoscale coastal circulations a synoptic-scale front will interact with them.

The modification of a cold front at the coast depends on the angles between front, coastline and prefrontal geostrophic wind. Garratt (1986) describes the modification of summertime cold fronts which are aligned perpendicular to the south coast of Australia and encounter a well-mixed hot air mass in their northern part over the land and a stratified cooler air mass with a strong surface inversion in their southern part over the sea. This leads to an acceleration and a channelling of the cold air near the coastline over the sea and thus to a distortion of the frontal line. These observational findings are confirmed by three-dimensional numerical simulations of gravity current-like fronts (Garratt et al., 1989). Another coastal effect in connection with a cold front aligned perpendicular to the east coast of the United States is described by Hakim (1992). Behind the southward moving cold front a new front, called side-door front, develops from a sea-breeze front and penetrates further inland.

Physick (1988) reports on the modification of a cold front aligned parallel to the coast of southern Australia. The front is modified by a prefrontal trough over the land. Numerical simulations show that the mesoscale trough develops over the heated land due to the sea-land temperature contrast. The synoptic-scale front is accelerated into the trough and the two features merge to form a new front.

In this paper we present a case study of a synoptic-scale front which interacted with a sea-breeze front at the German North Sea coast. Observations over the sea, at the coast and over the land are used to analyse the main characteristics associated with the synoptic-scale front over the sea before the interaction, the interaction processes between synoptic-scale and sea-breeze front near the coast, and the consequences of the interaction. The front case presented here was observed on 9 May 1989 during the field experiment FRONTEX 1989 which took place from 3 May to 6 June 1989 over the German Bight and Northern Germany (Brümmer, 1990; Hennemuth et al., 1991). On that day a coast-parallel cold front passed the German North Sea coast approximately at noon. The prefrontal geostrophic wind was nearly parallel to the front and favoured the development of a sea-land breeze. The synoptic-scale front was rather weak over the sea and interacted with the sea-breeze front near the coastline. By this interaction the front experienced a mesoscale strengthening in the boundary layer. The orientation of the synoptic-scale front with respect to the coastline and the time of the coastal passage were essential conditions for this modification. Numerical simulations closely following the observational findings are presented in a companion paper by Rhodin (1995).

2. Synoptic-scale conditions

The frontal cloud systems as seen by the NOAA-11 satellite at 0845, 1156 and 1337 UT on 9 May 1989 are presented in Figs. 1(a–c). A 200 km wide cloud band marked by "A" extended from Denmark across the North Sea to England and approached the coast of Northern Germany and The Netherlands. In the course of the time the cloud band "A" became smaller and reduced its cross-frontal propagation speed. Ahead of and parallel to "A" was a cloud band marked by "B" which was about 20 km wide and extended over several hundred kilometers. The cloud structures of "B" also weakened as the front moved on. At 1337 UT residues of "B" were situated over the middle of Schleswig–Holstein.

In the course of the morning, cumulus convection developed over land. The clouds were arranged in streets parallel to the mean prefrontal wind which was approximately parallel to the front. At 1337 UT a 20–30 km wide compact cloud band which developed from the cloud streets near the coast lay already 40 km inland followed by a 70 km wide cloud gap. The cloud band is marked by "C". It moved further inland in the course of the time and reached the region of Berlin in the late evening hours with rain. It will be shown below

(a)

(b)

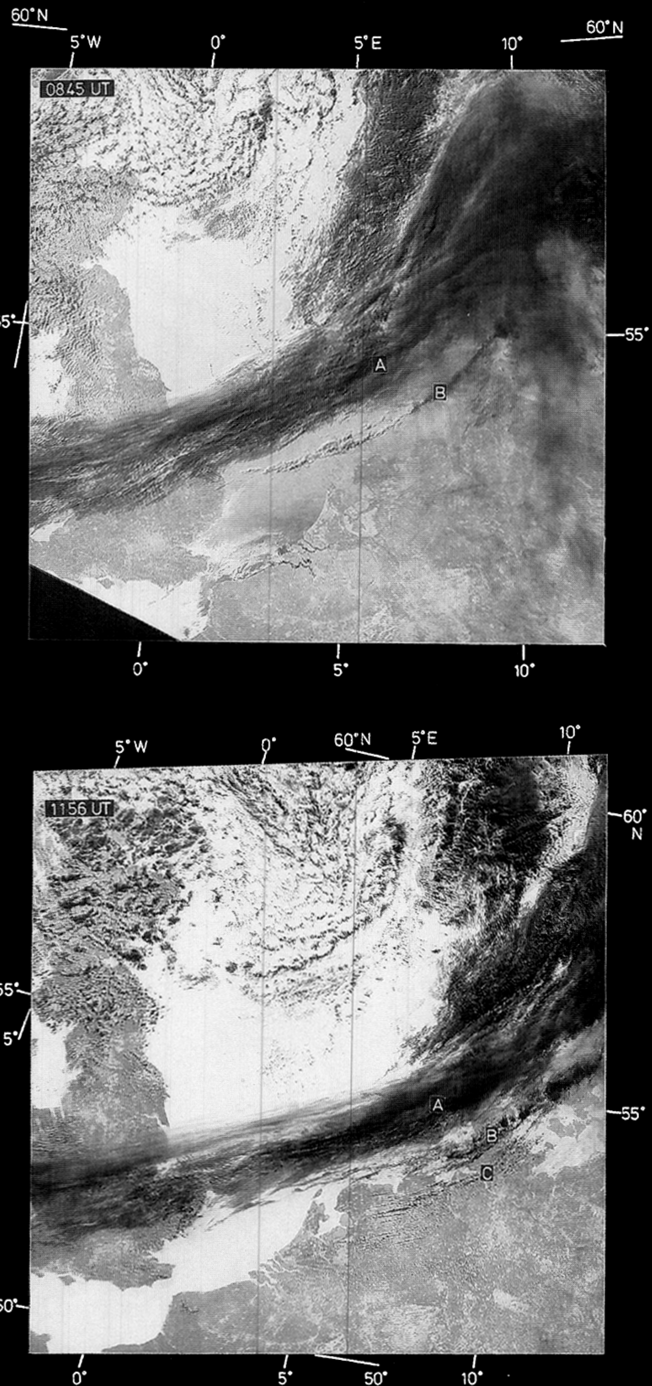

Fig. 1. NOAA-11 satellite images (visible channel 1) on 9 May 1989 at 0845 UT (a), 1156 UT (b), and 1337 UT (c). By courtesy of the University of Dundee. Letters A, B, and C mark respective cloud bands.

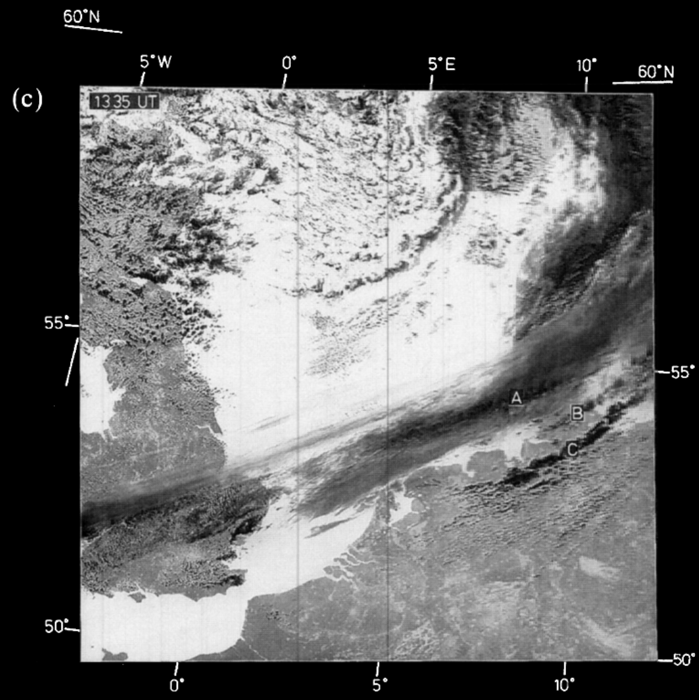

Fig. 1. (cont'd)

that the frontal contrasts of temperature, moisture and wind over the sea were associated with the cloud systems "B" and "A" and over the land with cloud band "C".

Half-hourly METEOSAT satellite images between 08 and 16 UT (not shown) are used to estimate the propagation speed of the cold front from positions of the respective cloud bands. Knowing that this procedure is not very accurate due to the coarse spatial resolution of the METEOSAT images at 55° N we estimate a nearly constant cross-frontal propagation speed of 5 m/s for cloud band "A" and of 4 m/s for cloud band "B". In the afternoon "A" seems to become slower because it partly dissolved at its front side. At noon when the front appears to jump from "B" to "C" a virtual propagation speed of 10 m/s is obtained. There upon the cloud band "C" propagated at a speed of 7 m/s and in the late afternoon at a speed of 5 m/s. We assume 6 m/s as a mean frontal speed for the period 08–16 UT. The mean orientation of the front was 60° against North.

Analyses based on the T 106 model version of the European Center for Medium-Range Weather Forecast (ECMWF) are used to describe the large-scale environment in which the frontal processes were embedded. Fig. 2 shows the distributions of geopotential height z and potential temperature Θ at 1000 and 850 hPa at 06 and 12 UT, respectively. The positions of the surface front are marked according to the surface analyses of the German Weather Service. At 1000 hPa, the temperature contrast across the front in the North Sea region was small at 06 UT but intensified considerably until 12 UT. This was due to the heating of the prefrontal air over the land. At 12 UT the frontal temperature gradient was maximum in the region of the German and Dutch coast with a value of about 12 K over a distance of 250 km. The frontal temperature contrast at 850 hPa was stronger than at the surface at 06 UT, but it encountered no intensification in the course of the day.

Vertical cross-sections of potential temperature Θ, specific humidity q and along-front wind component v (positive when directed towards low pressure) across the front at 06 and 12 UT are displayed Fig. 3. They are calculated from the ECMWF analyses and hold for the line A–B

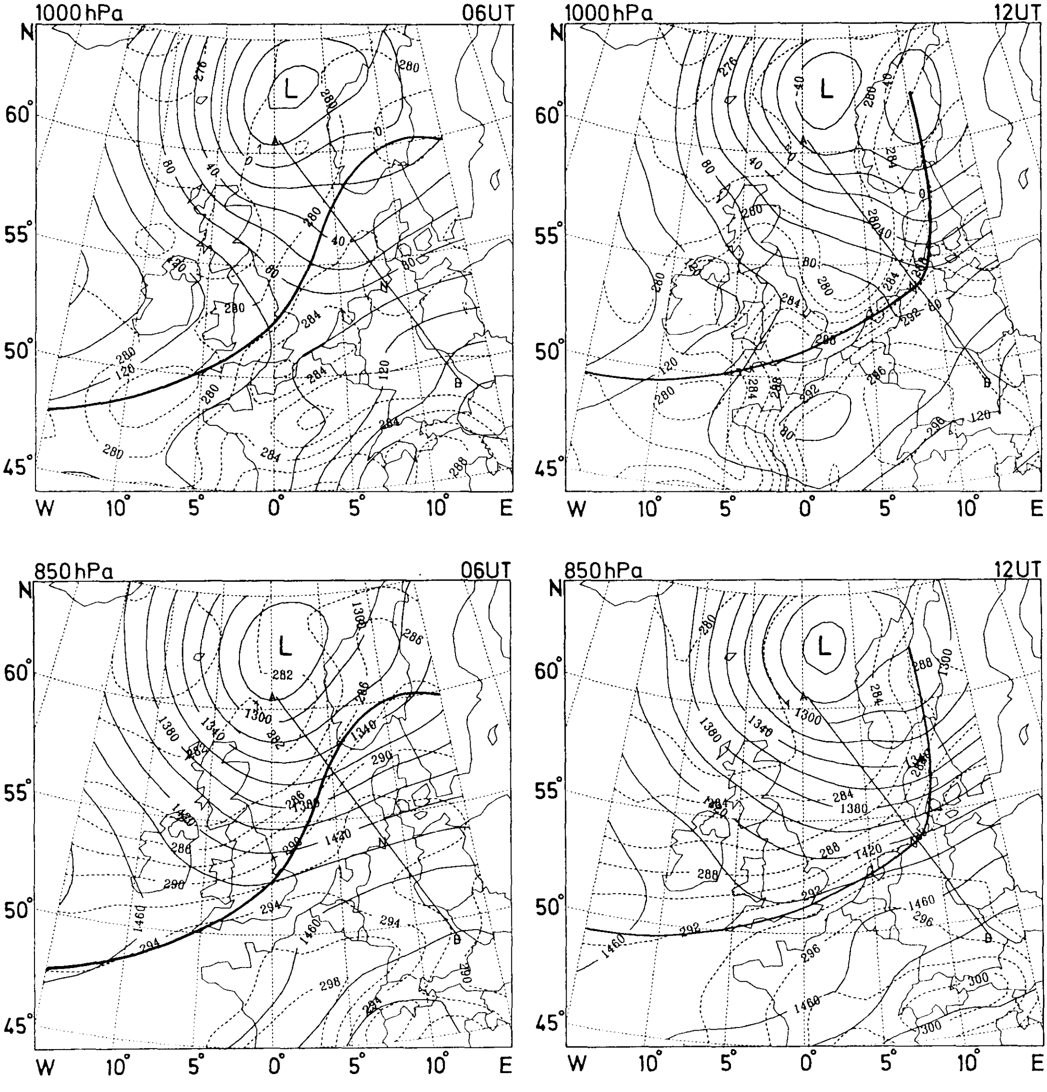

Fig. 2. ECMWF T106 analyses of geopotential height (in meters, full lines) and potential temperature (in K, dashed) on 9 May 1989 at 06 and 12 UT at 1000 and 850 hPa. Line A–B denotes position of vertical cross-sections in Fig. 3. Thick line marks the position of the surface front according to analysis of the German Weather Service.

marked in Fig. 2. They also show that the frontal temperature contrast in the boundary layer was weak at 06 UT and increased to a considerable magnitude at 12 UT. The field of specific humidity was characterized by high q values ahead and above the frontal temperature gradient zone. The front-parallel v wind component had its absolute maximum at the inclined tropopause over the northern part of the North Sea; an axis of relative maxima extended downward to a position ahead of the surface front.

In order to assess whether the large-scale fields of temperature and geostrophic wind support or hinder a cross-front ageostrophic circulation the so-called $\boldsymbol{Q}$-vector,

$$\boldsymbol{Q}=\left(-\frac{\partial \boldsymbol{v}_{\mathrm{G}}}{\partial x}\nabla_{\mathrm{p}}\Theta,\ -\frac{\partial \boldsymbol{v}_{\mathrm{G}}}{\partial y}\nabla_{\mathrm{p}}\Theta\right), \tag{1}$$

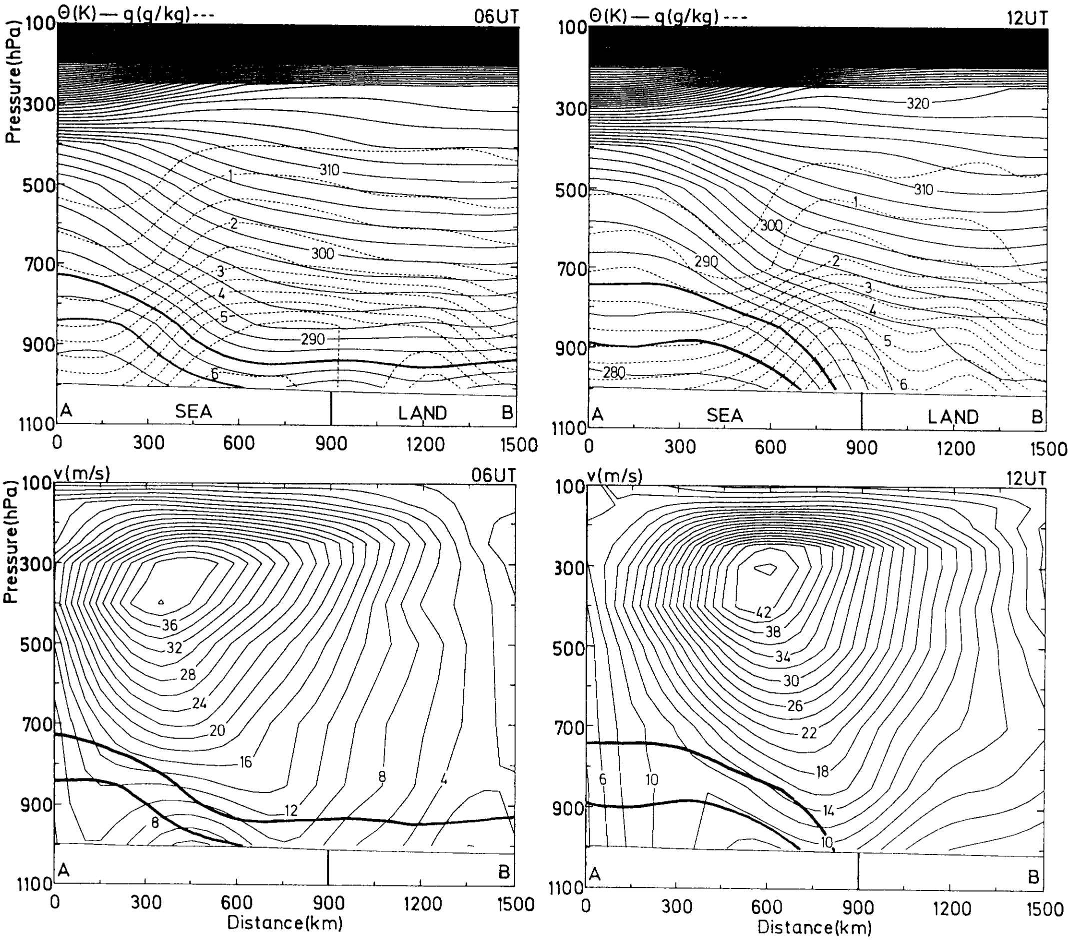

Fig. 3. Vertical cross-sections of potential temperature Θ, specific humidity q, and along-front wind component v at 06 and 12 UT, respectively, from ECMWF analysis data along line A–B marked in Fig. 2.

was computed from the ECMWF analysis at 12 UT. In (1) $\mathbf{v}_G$ is the geostrophic wind vector, $\nabla_p \Theta$ is the potential temperature gradient on a pressure surface, and x and y are the horizontal axes of the cartesian coordinate system whose x axis is directed normal to the front from the cold to the warm side. $\boldsymbol{Q}$ can be partitioned into a part $\boldsymbol{Q}_n$ normal to the isentropes representing an increase or decrease of the magnitude of the temperature gradient and into another part $\boldsymbol{Q}_s$ parallel to the isentropes representing a change of the direction of the temperature gradient (Keyser et al., 1992; Kurz, 1992). Divergence or convergence of the $\boldsymbol{Q}$-vector is identical with the forcing of downward or upward vertical motions according to the ω-equation (Hoskins et al., 1978) and thus the convergence of $\boldsymbol{Q}_n$ describes the forcing of ascent along the front. Fig. 4 shows the fields of div $\boldsymbol{Q}_n$ and relative humidity at 850 hPa on 9 May 1989 at 12 UT. The regions of maximum convergence of $\boldsymbol{Q}_n$ nearly coincide with the regions of maximum relative humidity. Thus it may be concluded that the broad frontal cloud band "A" over the sea is due to geostrophically forced ascent of moist air.

Due to its coarse spatial resolution, the T 106 model analysis is not able to distinguish between synoptic-scale front and sea-breeze front and only shows a strong modification of a propagating

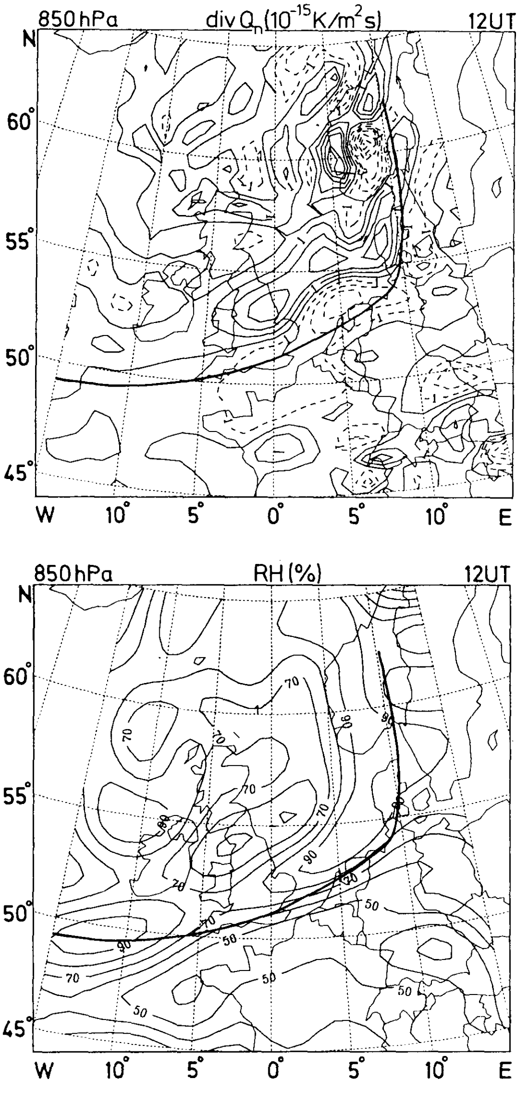

Fig. 4. Fields of div $\boldsymbol{Q}_n$ and relative humidity RH at 850 hPa on 9 May 1989 at 12 UT from ECMWF T106 analyses. Dashed lines of div $\boldsymbol{Q}_n$ indicate convergence and thus forcing of upward motion. Thick line marks the position of the surface front according to analysis of the German Weather Service.

front. The existence of two separate systems, however, can be concluded from the surface pressure and temperature fields analysed from the 12 UT SYNOP observations and presented in Fig. 5. A weak but well defined trough of low pressure was situated over North-Germany about 50 km inland. The zone of maximum potential temperature gradients lay between the trough axis and the coastline. The positions of the cloud systems "A", "B" and "C" taken from Fig. 1b are also shown in Fig. 5. Cloud band "C" with strong cumulus convection approximately coincides with the weak trough which apparently developed over the heated land in connection with the sea-breeze circulation. The numerical simulations of Physick (1988) show a similar situation with a mesoscale trough and a strong baroclinic zone about 60 km inland ahead of the approaching front.

3. Mesoscale structure of the cold front

During the FRONTEX 1989 campaign special measurements were made over sea and land using surface stations, radiosondes and aircraft; the locations are shown in Fig. 6. A spatially and temporarily continuous documentation of the development of the synoptic-scale front and sea-breeze front and the interaction of both fronts, however, is not possible due to the limitations of the available observational tools and also to the unforeseen and unforeseeable weather development. For example, when the aircraft missions were planned in the morning of 9 May 1989, the large-scale front was still far over the sea and the sea-breeze front had not yet evolved. Thus, the aircraft operations concentrated on the synoptic-scale front. When the aircraft returned from their missions to the operation base at Nordholz in the early afternoon, the sea-breeze front had passed already this station and the implication of this event was not assessed at that time. Therefore, the observations only can describe the frontal manifestation at different locations.

3.1. The front over the sea surface

The manifestation of the frontal passage in the surface layer at the most seaward located station, research platform FPN, which is situated about 140 km off the coast in cross-frontal direction is presented in Fig. 7.

During the period of constant pressure fall until 0500 UT ahead of the front, temperature T and along-frontal wind component v increased, a tendency which fits well to the ECMWF analysis in Fig. 3 where the v maximum extends downwards to the warm side of the front. The pressure

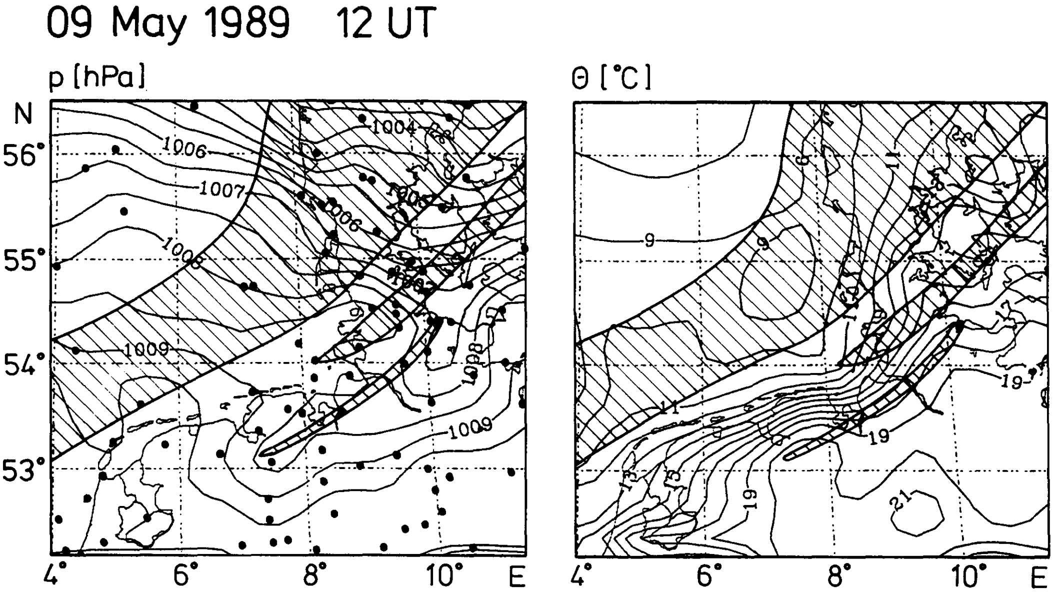

Fig. 5. Surface pressure p and potential air temperature Θ on 9 May 1989 at 12 UT from SYNOP data. Dots mark SYNOP stations and hatched areas mark positions of cloud bands A, B, C taken from Fig. 1.

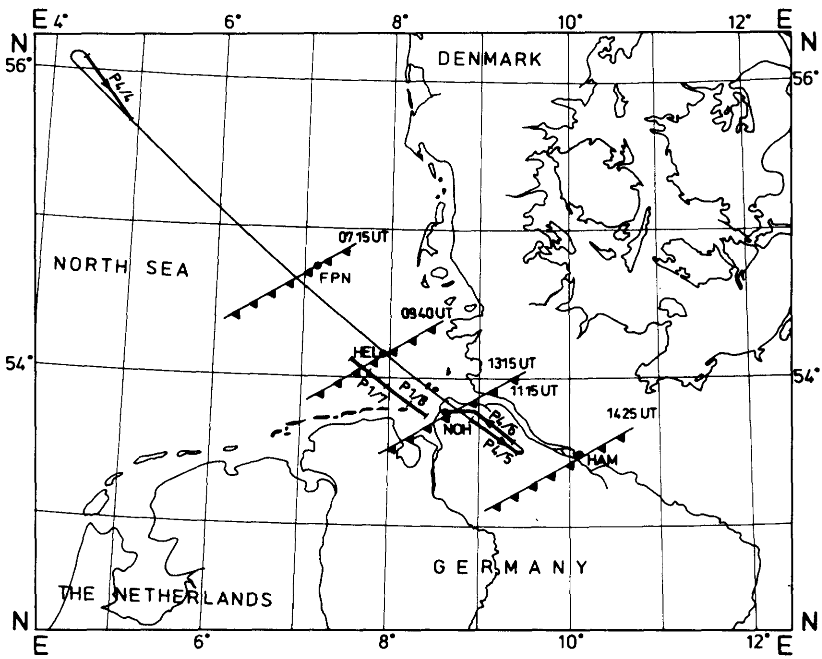

Fig. 6. Location of FRONTEX measurement stations (full circles) used in this paper: research platform FPN, isle of Helgoland (HEL), airfield Nordholz (NOH), and broadcasting tower at Hamburg-Billwerder (HAM), with corresponding times of frontal passage. For Nordholz passage times of synoptic-scale front and sea-breeze front are given. The flight pattern of research aircraft Polar 4 (P4) is marked by a thin line; research aircraft Polar 1 (P1) flew parallel and west of P4. Vertical sounding sections P4/4, P4/5, P4/6 of Polar 4 and P1/7, P1/8 of Polar 1 which are displayed in Fig. 12 are labelled.

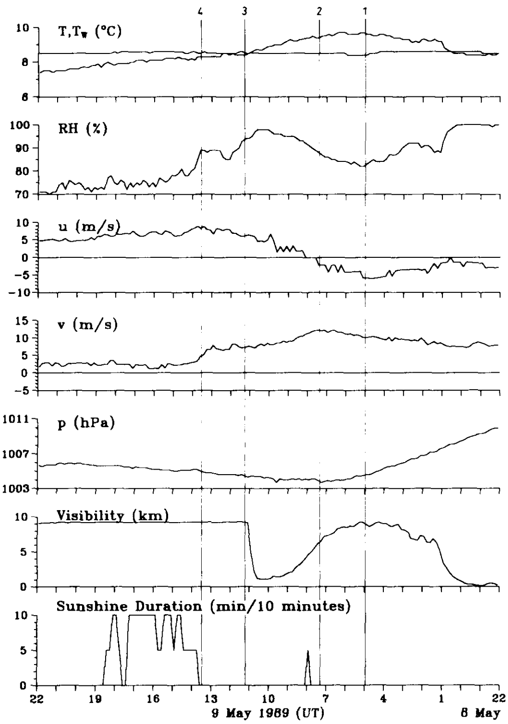

Fig. 7. Time series of 10 min averages of air temperature T, water temperature T_W, relative humidity RH, cross-front wind component u, along-front wind component v, pressure p, visibility and sunshine duration measured at reasearch platform FPN from 8 May 1989 22 UT to 9 May 1989 22 UT. Vertical lines denote: 1: end of continuous pressure fall, 2: pressure minimum, 3: increase of visibility, 4: begin of sunshine.

p reached its absolute minimum at 0715 UT indicating the arrival of the surface front. After that the along-front wind began to veer while T and visibility VIS decreased and relative humidity RH and cross-frontal wind component u increased. These tendencies continued during the next hours. Between 1040 and 1110 UT, VIS increased rapidly at the same time when the air-sea temperature difference changed from stable to unstable and u exceeded the frontal speed of 6 m/s. At 1330 UT beginning sunshine indicates the rear side of cloud system "A" (see Fig. 1c). This event was connected with the sharpest veering of the wind during the frontal passage.

The records at FPN show that the frontal changes over the sea occurred in a broad zone. The temperature decreased over 7 h within the "cloud zone" and continued to decrease in the cold air. Also the cyclonic shear of v as well as the confluence of u lasted over 6 and 8 h, respectively. This corresponds to horizontal distances of approximately 130 and 170 km, respectively, if time intervals Δt are converted to distances Δx via the relation

$$\Delta x = c_F \, \Delta t, \tag{2}$$

where c_F is the frontal propagation speed which is assumed as 6 m/s.

The vertical structure of the cold front over the sea was documented by means of three-hourly radiosonde ascents at the isle of Helgoland between 00 UT on 9 May 1989 and 12 UT on 10 May 1989 and by aircraft traverses through the front between Nordholz and the position 56°N, 04°E during the period 0845 until 1215 UT (see Fig. 6). Converting time intervals to distances according to (2), the radiosonde measurements represent a 780 km wide cross-section around the front, while the aircraft measurements represent a 400 km wide cross-section (Fig. 9). For comparison: the ECMWF analyses in Fig. 3 represent a 1500 km wide cross-section. Thus, the width of the horizontal domains of the cross-sections in Figs. 3, 8 and 9 differ by the factor two from each other.

The isle of Helgoland is situated about 55 km off the coast in cross-frontal direction. The leading edge of the frontal zone, as given by the pressure minimum, reached Helgoland at about 0940 UT. The time-height cross-sections of Θ, q, u and v are displayed in Fig. 8. The gross features of the vertical structure are similar to the ECMWF analyses at 06 UT in Fig. 3. The inclined frontal transition zone characterized for example by the isentropes Θ of 14°C and 10°C leveled off at the leading side and merged with a prefrontal low-level inversion. This zone coincides with the zone of large vertical v shear as to be expected from the thermal wind equation. The v maximum extended downward from higher levels; the largest v values in the boundary layer were observed between 06 and 09 UT ahead of the surface front. The front had a very pronounced moisture structure with high values ahead and on top of the frontal transition zone and a tongue of low values below the frontal zone. This, together with the structure of the cross-frontal wind component, suggests a cross-frontal

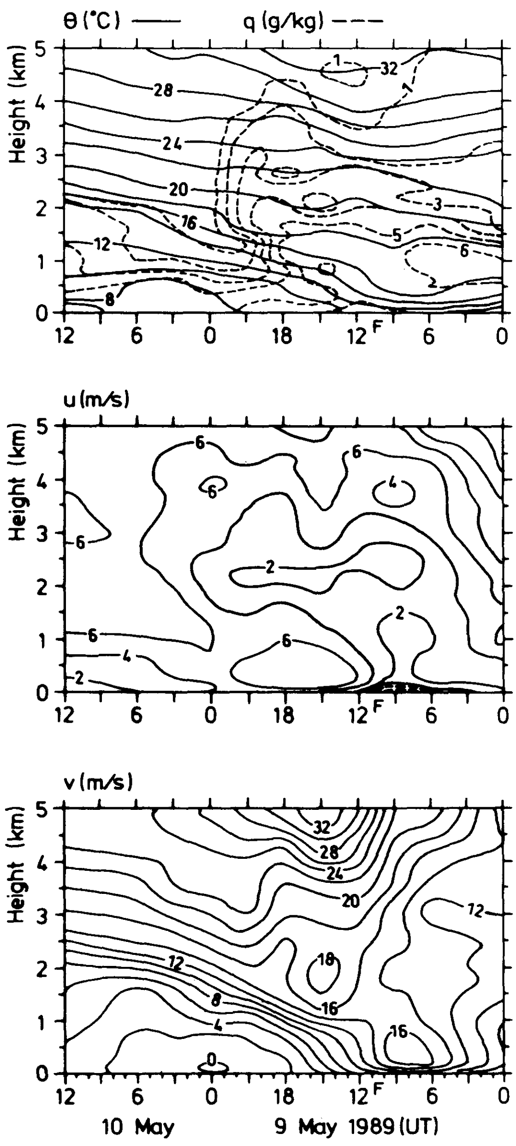

Fig. 8. Time-height cross-sections of potential temperature Θ, specific humidity q, cross-front wind component u, along-front wind component v based on three-hourly radiosoundings at the isle of Helgoland. Letter F marks frontal passage.

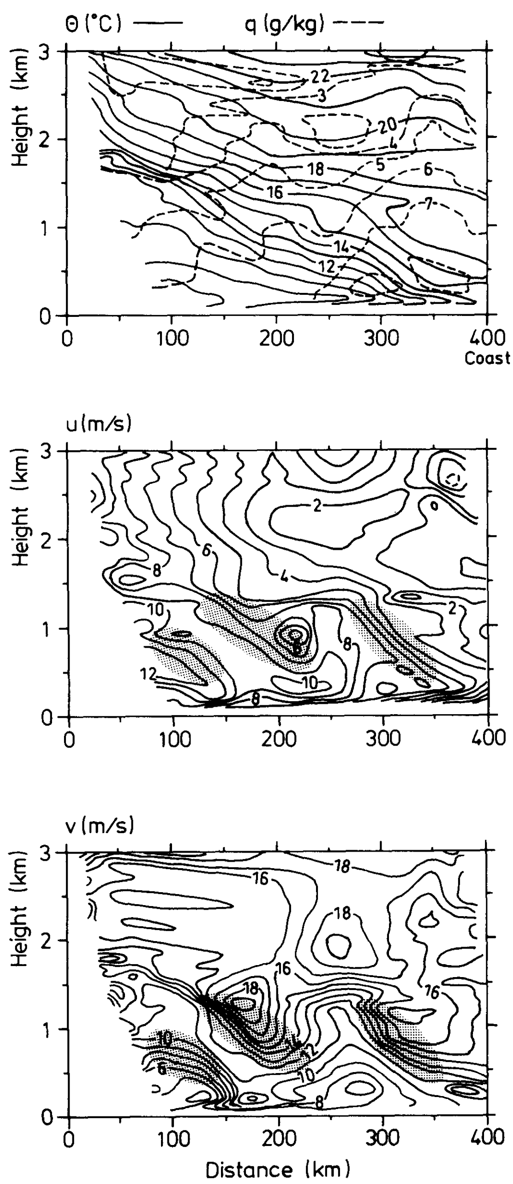

Fig. 9. Vertical cross-sections of potential temperature Θ, specific humidity q, cross-front wind component u, along-front wind component v through the synoptic-scale front over the sea based on measurements of reasearch aircraft Polar 1 and Polar 4 on 9 May 1989 between about 09 and 12 UT along the flight pattern shown in Fig. 6 (except that part which was flown over land). The abszissa represents horizontal distance relative to the moving front; the origin is arbitrarily chosen. The coastline is around 400 km.

circulation with ascending warm and moist air ahead of the frontal inversion and descending cool and dry air 250 km behind the frontal inversion. Taking the $\Theta = 14°C$ isoline as a reference, the frontal inclination was not very steep (about 2 km rise over a distance of about 500 km) and also the vertical extension of clouds was not very high (about 4 km). Thus, the convective activity at the front was relatively weak, although the frontal circulation was clearly organized. When the front reached Helgoland at about 0940 UT, the sea-breeze was not yet established, so that no frontogenic feed-back occurred at this time and this location. On the contrary, the low-level u maximum behind the front was only about 6 m/s at Helgoland compared to 9 m/s at FPN. This suggests that the front was generally in a weakening stage in accordance with the cloud development (cloud bands "A" and "B") visible on the NOAA satellite images in Fig. 1.

Details of the mesoscale structure of the frontal zone over the sea were obtained from two meteorologically equipped research aircraft, called Polar 1 and Polar 4, which flew in formation forth and back through the front at heights of 150, 250, 900 and 1500 m. The flight pattern is shown in Fig. 6 and was approximately oriented along the line A–B of Fig. 2. At the beginning and at the end of the horizontal tracks vertical soundings were performed up to 3000 m. The airplanes started at 0845 UT from Nordholz before the front reached the coast, flew through the frontal cloud bands "A" and "B", turned in the cloudless area behind "A" and landed at 1215 UT between the cloud systems "B" and "C".

Cross-sections in the cross-frontal $x-z$-plane are constructed from the aircraft measurements, excluding the landing profiles. An average frontal speed of 6 m/s was used in order to compose the data from the forth and back flights into the cross-sections in Fig. 9. There, the horizontal coordinate x is given in units relative to the moving front. The origin $x=0$ represents an arbitrary point over the sea. In such a coordinate system an earth-fixed point like the coast becomes a line with the length $\Delta x = c_F \, \Delta t$. Thus, the Δx-range named "Coast" in Fig. 9 marks the position of the coast at the beginning and end of the aircraft traverses.

The core region of the frontal temperature transition zone was between the isolines $\Theta = 10°C$ and $\Theta = 14°C$. Due to the fine horizontal resolutions ($\Delta x = 1$ km) much more details of the frontal structure are visible in Fig. 9 than in the cross-sections in Fig. 3 based on the ECMWF data (Δx about 100 km) and in Fig. 8 based on the radiosonde ascents (Δx about 65 km). The transition from large moisture values ahead of the front to small values behind the front occurred in several steps (identified for example by the 6 g/kg-specific humidity isoline in Fig. 9). The first and highest plume was associated with cloud band "B". The following two smaller moisture plumes were associated with substructures embedded in cloud system "A". The moisture structures were connected with zones of u-confluence, $\partial u/\partial x < 0$, and cyclonic v-shear, $\partial v/\partial x > 0$ (marked by the hatched areas in Fig. 9).

The moisture structures have horizontal scales about of 50 km and resemble the wide cold frontal rainbands described by Houze and Hobbs (1982). A possible mechanism for the generation of such band-like structures in frontal zones is given by the conditional symmetric instability (CSI) (Emanuel, 1983). The criterion for CSI is a positive equivalent potential vorticity,

$$p_e > 0 \tag{3a}$$

with

$$p_e = \frac{1}{\rho g}\left(\frac{\partial m}{\partial x}\frac{\partial \Theta_e}{\partial z} - \frac{\partial \Theta_e}{\partial x}\frac{\partial m}{\partial z}\right). \tag{3b}$$

In (3b) Θ_e is the equivalent potential temperature, $m = u + fx$ is the absolute momentum and f is the Coriolis parameter. Criterion (3a) for CSI holds in wide areas of the frontal zone (not shown).

3.2. *The front near the coast*

The evolving sea-breeze front and the synoptic-scale front near the coast are documented by measurements at stations near the coast and by vertical aircraft soundings.

Fig. 10 shows the meteorological conditions recorded at the airfield Nordholz which is situated about 7 km inland. The period of constant pressure fall ended at 1030 UT. From now on the wind began to veer due to an increase of the cross-frontal wind component u. 45 minutes later, the temperature decreased, the humidity increased and the wind veered (increase of u component and decrease of v component) in a stepwise manner. This time marked the passage of the sea-breeze front at Nordholz advecting cool and moist air from the sea. Due to solar heating of the land surface the prefrontal air reached temperature

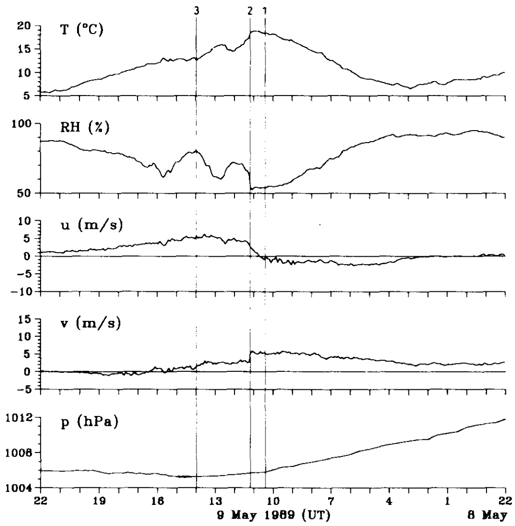

Fig. 10. Time series of 1 min averages of temperature T, relative humidity RH, cross-front wind component u, along-front wind component v, and pressure p at Nordholz between 22 UT on 8 May and 22 UT on 9 May 1989. Vertical lines denote: 1: end of nearly constant pressure fall, 2: passage of sea-breeze front, 3: moisture maximum associated with cloud band "B".

values of 19°C. This is about 10 K warmer than in the prefrontal air at research platform FPN.

A second temperature decrease and a second moisture increase were observed between 13 and 14 UT. These changes were connected with the arrival of cloud band "B" (see Fig. 1c). Although the clouds within cloud band "B" had already dissolved over Nordholz at this time, their former existence was still manifested in a zone of higher moisture values. Only a small v shear marked the passage of band "B" in the wind field. No significant confluence of the cross-front wind component u was present. This appears to be a result of the recently evolved sea-breeze front which led on its seaward side to an increase of the u wind. Thus, an important front-maintaining process, the fluence frontogenesis $(\partial u/\partial x)(\partial \Theta/\partial x)$, is absent at cloud band "B", the leading edge of the synoptic-scale cold front. Strong fluence frontogenesis is now present at the sea-breeze front, instead. When the synoptic-scale front was over the sea, it was still associated with considerable confluence $\partial u/\partial x$ (see Fig. 7).

Wind measurements in the lowest 500 m of the atmosphere were made by a SODAR system at Nordholz (Fig. 11). They show that the above-mentioned wind changes associated with the sea-breeze front and the synoptic-scale front occurred nearly simultaneously in a 200 to 300 m thick layer above the surface. Above this layer, both frontal zones were inclined with height towards the colder air. The synoptic-scale front is almost not discernible in the cross-section of the u component; nearly the entire u confluence is concentrated at the sea-breeze front. The situation is a different one for the v component: the zones of increased v shear, $\partial v/\partial x$, are still discernible for either front. However, the facts that the maximum $\partial v/\partial x$ occurs below 200 m with the sea-breeze front and above 200 m with the synoptic-scale front and that the v isolines for 4, 6 and 8 m/s have a tongue-like structure extending at the lower levels from the synoptic-scale front to the sea-breeze front hint to an interaction and a re-organization of both fronts which is just taking place.

When research aircraft Polar 4 returned from its mission over the sea, it intersected rather accidently the sea-breeze front because (as mentioned at the beginning of Section 3) the existence of a sea-breeze front was unknown during the flight. Instead of landing directly at Nordholz between cloud bands "B" and "C", Polar 4 prolonged its 250 m level flight over the sea for about 40 km in inland direction, descended shortly to 100 m height and made a profile ascent to 3 km height keeping always the same heading. After turning at 3 km height it descended in several steps to the airfield Nordholz (see Fig. 6). It turned out later, that the ascent profile, termed P4/5, took place just ahead of the sea-breeze front and the descent profile, termed P4/6, was flown through the sea-breeze front.

The cold air behind the sea-breeze front had a depth of about 450 m at this particular location (Fig. 12). At the surface it was about 4 to 5 K colder than the air ahead of the front which was well-mixed up to about 1500 m height. In qualitative accordance with the thermal wind equation,

$$\frac{\partial v_g}{\partial z} = \frac{g}{f\Theta} \frac{\partial \Theta}{\partial x}, \tag{4}$$

a sharp vertical wind shear $\partial v/\partial z$ was present at the top of the tilted sea-breeze frontal inversion. This

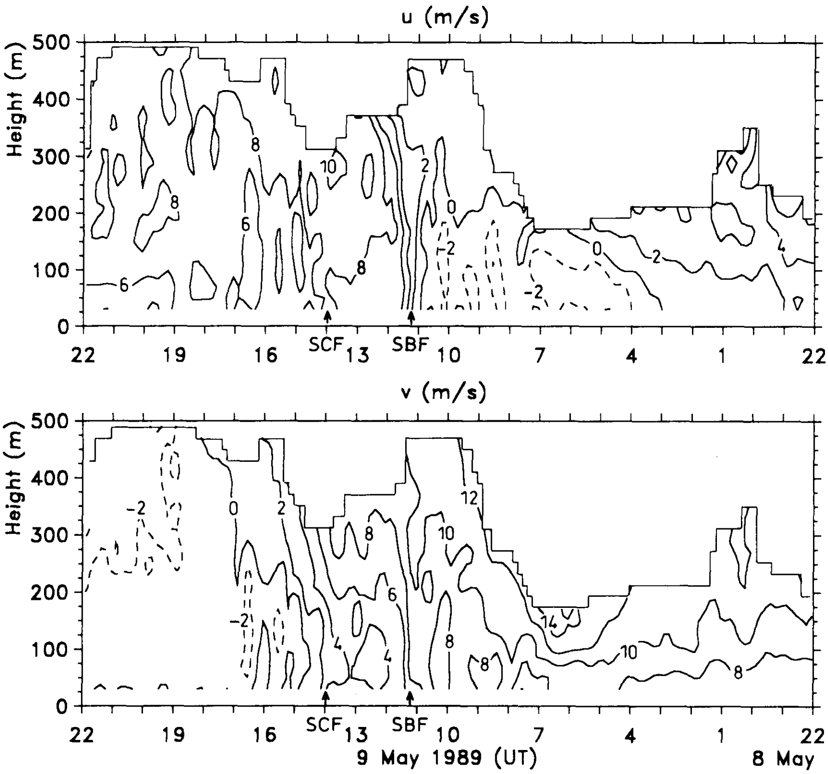

Fig. 11. Time-height cross-sections of cross-front wind component u and along-front wind component v measured by a SODAR system at Nordholz between 22 UT on 8 May and 22 UT on 9 May 1989. "SFB" and "SCF" mark the sea-breeze front and synoptic-scale front, respectively.

resulted in a strong cyclonic shear $\partial v/\partial x$ in the lowest 450 m. The cross-frontal wind component u showed a jet-like structure in the cold air causing a u confluence at the sea-breeze front. Since the ascent profile was measured immediately ahead of the sea-breeze front, only a part of the total u confluence is reflected in Fig. 12. The records at Nordholz in Fig. 10 show that u began to increase already one hour (corresponding to about 22 km distance according to (2)) before the sea-breeze front arrived.

During the ascent profile P4/5, several clouds within cloud band "C" were intersected. They were of type "cumulus congestus"; their bases ranged between 1200 and 1400 m height and their tops between 2500 and levels higher than the highest flight level of 3100 m. Thus, the convection at the sea-breeze front had a similar depth as that at the synoptic-scale front.

For comparison with profiles P4/5 and P4/6, three additional aircraft soundings measured over the sea (for location see Fig. 6) are displayed in Fig. 12. Profiles P1/7 (ascent) and P1/8 (descent) measured by research aircraft Polar 1 represent the conditions around the synoptic-scale front in the region between the coast and Helgoland. Remarkable features are the low-level inversion as well as the diffluent u wind field and anticyclonic v wind shear across the synoptic-scale front below the inversion. The absence of confluence across the synoptic-scale front agrees with the observations at Nordholz (see Fig. 10). Profile P4/4 (descent) in Fig. 12 characterizes the conditions in the cloudless air about 300 km behind the synoptic-scale surface front. There, the cold air mass is about 1600 m deep, very dry and moves with relatively high cross-front wind u towards the surface front. These are favourable conditions to

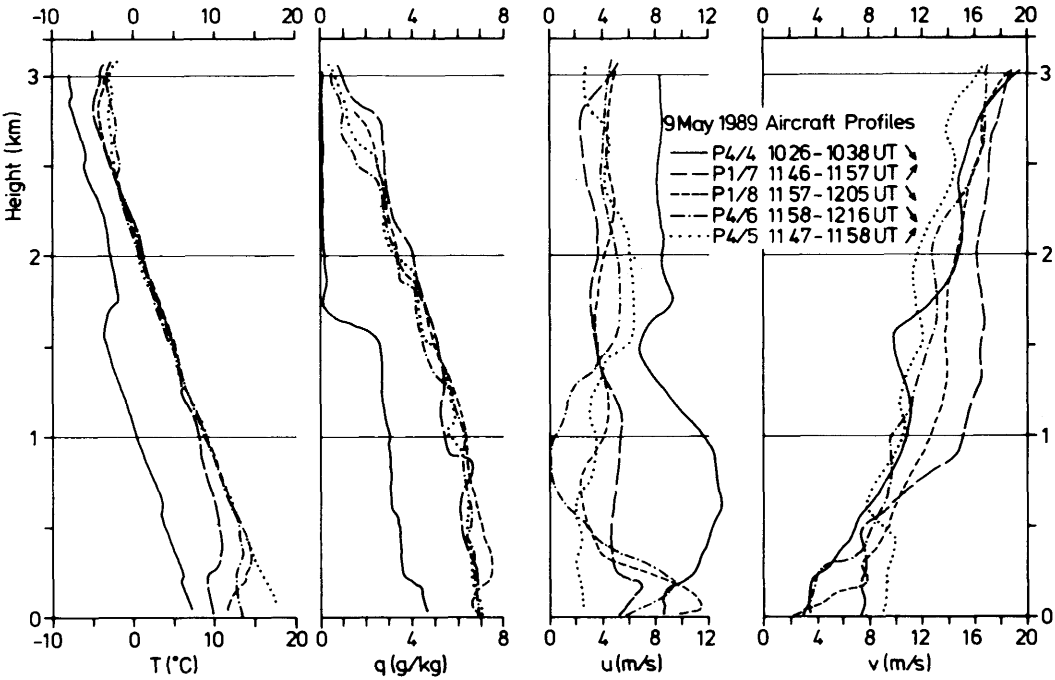

Fig. 12. Vertical profiles of temperature T, specific humidity q, cross-front wind component u, and along-front wind component v measured by research aircraft Polar 1 (P1) and Polar 4 (P4). See Fig. 6 for location of measurements: profiles P4/5 and P4/6 were flown ahead of and through the sea-breeze front, respectively, profiles P1/8, P1/7 and P4/4 ahead of, closely behind, and about 300 km behind the synoptic-scale front, respectively.

maintain the general frontal contrast on a larger scale between the deep cold air pool and the warm air ahead of the sea-breeze front.

Taken together, the measurements near the coast resolve two frontal structures at the surface: a strong and sharp sea-breeze front ahead of the weak and weakening synoptic-scale cold front.

3.3. *The front further inland*

The characteristics of the front at about 80 km distance from the coast can be understood from Fig. 13 which presents time series of several meteorological parameters recorded at 50 m height at the broadcasting tower in Hamburg-Billwerder. During the frontal passage which was associated with cloud band "C" all parameters changed simultaneously between 1425 UT and 1450 UT in a nearly step-wise manner: temperature dropped by 2.5 K, relative humidity increased by 20%, cross-frontal wind increased by 10 m/s, along-frontal wind decreased by 7 m/s and pressure increased by about 0.4 hPa. These frontal changes are not dramatic, however, they are remarkable in two respects. First, the double frontal structure, observed at the coast with some hints of an ongoing re-organization, has changed to a single frontal structure with all frontal characteristics now concentrated at cloud band "C", the former sea-breeze front. Second, the interaction between synoptic-scale front and sea-breeze front resulted in a modification of a weak and broad frontal zone over the sea to a strong and sharp frontal zone over the land, i.e., in an intensification of the synoptic-scale front.

The only information about the vertical structure of the front over the land is available from the measurements at 6 levels (10, 50, 70, 110, 175, 250 m) at the broadcasting tower. Fig. 14 shows that the frontal changes occurred almost simultaneously (the time resolution of the data is 5 min) in the lowest 250 m. The main part of the frontal changes took place during a period of only

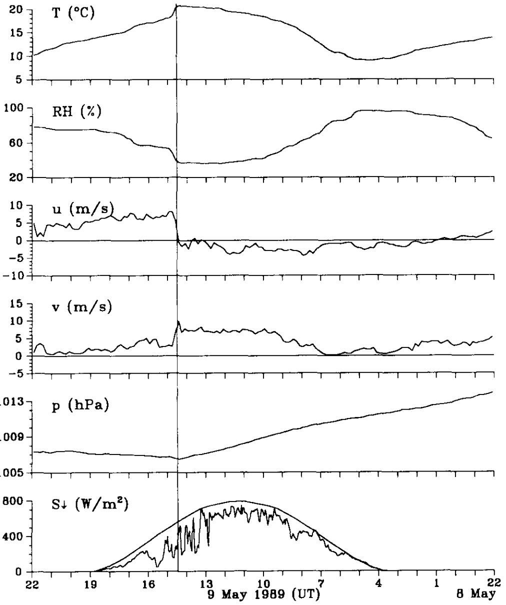

Fig. 13. Time series of 5 min averages of temperature T, relative humidity RH, cross-front wind component u, along-front wind component v at 50 m height, surface pressure p, and global radiation $S\downarrow$ measured at the broadcasting tower in Hamburg-Billwerder between 22 UT on 8 May and 22 UT on 9 May 1989. The smooth S curve represents global radiation in a cloudless atmosphere. The vertical line marks the frontal passage.

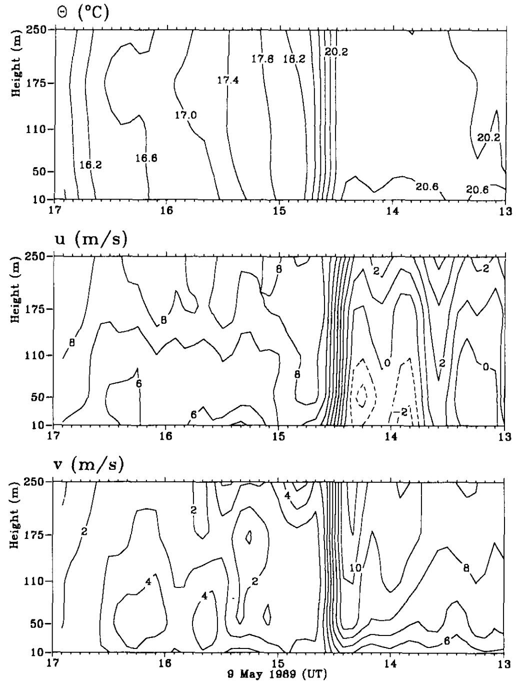

Fig. 14. Time-height cross-section of potential temperature Θ, cross-front wind component u, and along-front wind component v based on measurements at 10, 50, 70, 110, 175, and 250 m height at the broadcasting tower in Hamburg-Billwerder between 13 and 17 UT on 9 May 1989.

10 min. The vertical cross-sections of u and v show relatively narrow zones of extreme values immediately ahead and behind the frontal gradient zone, which were embedded in the general cross-frontal contrasts of both wind components to be seen in Fig. 13. Such features are typical for sharp cold fronts with a density-current-like character (Shapiro, 1984; Brümmer, 1988).

The tower height of 250 m is not sufficient to measure the depth h of the cold air behind the front. However, knowing from Fig. 14 that the temperature is well-mixed in and behind the front, h may be estimated from the pressure increase Δp caused by the replacement of the warmer air ahead of the front by the cooler air behind it. According to the hydrostatic equation the vertical pressure difference dp across a layer of depth h with the layer-averaged temperature $\bar{T}$ and pressure $\bar{p}$ is

$$\mathrm{d}p = \frac{g\bar{p}}{R\bar{T}} h. \tag{5}$$

If we derive (5) with respect to $\bar{T}$ and resolve for h, we obtain

$$h = \frac{R\bar{T}^2}{g\bar{p}} \frac{\Delta(\mathrm{d}p)}{\Delta T}, \tag{6}$$

where $\Delta(\mathrm{d}p) = \Delta p$ is the pressure increase and ΔT is the temperature decrease across the front. From Figs. 13 and 14 we take $\Delta p = 0.4$ hPa, $\Delta T = 2.5$ K for the period between 1425 UT and 1450 UT, $\bar{T} \approx 292$ K and $\bar{p} \approx 985$ hPa and thus estimate according to (6) a value of 404 m for the depth h of the cold air behind the front. This is about the same depth as observed for the sea-breeze front at Nordholz (Figs. 11 and 12). Thus it may be concluded that, as a result of the interaction between synoptic-scale front and sea-breeze front in the coastal region, the leading edge of the front over the land has overtaken the characteristics of the former sea-breeze front.

4. Concluding remarks

The modification of the synoptic-scale cold front by the interaction with the sea-breeze front can be quantified by the cross-frontal differences and gradients at different stages of the frontal development taken from the surface observations at FPN (Fig. 7), Nordholz (Fig. 10) and Hamburg-Billwerder (Fig. 13). The results are listed in Table 1. In order to convert time differences Δt to cross-frontal distances Δx according to (2) the same frontal speed c_F of 6 m/s has been used although c_F was not constant as will be discussed below. Also, it should be mentioned that the passage time (t_a) of the leading edge of the frontal zone can be determined with more certainty than the passage time (t_b) of the rear-side edge of the frontal zone. However, these uncertainties are not so large to cause principal changes of the results in Table 1. The frontal gradients at the synoptic-scale front are about one order of magnitude smaller than at the sea-breeze front. The fluence frontogenesis term, $(\Delta u/\Delta x)(\Delta T/\Delta x)$, shows that the synoptic-scale front was in a weakening stage on its way from FPN to Nordholz. Difluence at Nordholz, $\Delta u/\Delta x > 0$, even causes frontolysis,

$$-\frac{\Delta u}{\Delta x}\frac{\Delta T}{\Delta x} < 0,$$

there. On the other hand, the sea-breeze front shows strong fluence frontogenesis which even increased further inland when the sea-breeze front became the main front. Strong frontal gradients and strong fluence frontogenesis are a frequent feature of sea-breeze fronts (e.g., Kraus et al., 1990). Thus, the incorporation of the sea-breeze front into the general frontal circulations led to a re-intensification of the frontal zone at least at low levels.

This incorporation appears to be completed when the front reached Hamburg-Billwerder. This may be concluded from the surface pressure records at the various stations. The frontal passage at FPN and Helgoland occurred with the absolute pressure minimum. Near the coast, at Nordholz, two pressure minima were observed, a relative one with the passage of the sea-breeze front and the absolute one with the passage of the residues of the synoptic-scale front. Only 70 km further in positive cross-frontal direction, at Hamburg-Billwerder, and only three hours later the pressure field was adjusted in such a way that the absolute pressure minimum occurred with the leading edge of the frontal zone, the former sea-breeze front.

The frontal propagation speed c_F was estimated from satellite images (Section 2) and in addition from the frontal passage at different locations. The

Table 1. *Frontal modification calculated from the cross-frontal differences ahead (index (a)) minus behind (index (b)) the front at different locations*

Front	Location	t_a (UT)	t_b (UT)	Δt (min)	Δx (km)	T_a (°C)	T_b (°C)	ΔT (°C)	u_a (m/s)	u_b (m/s)	Δu (m/s)
synoptic-scale	FPN	0715	1330	375	135	9.5	8.3	1.2	−2.5	9.0	−11.5
front	Helgoland	0940	1500	320	115	12.0	9.0	3.0	0.0	5.0	−5.0
	Nordholz	1315	1640	205	75	15.5	12.0	3.5	6.0	3.5	2.5
sea-breeze	Nordholz	1115	1200	45	16	18.8	14.5	4.3	3.0	5.5	−2.5
front	Hamburg	1425	1445	20	7	20.8	18.3	2.5	−1.0	8.0	−9.0

Front	Location	v_a (m/s)	v_b (m/s)	Δv (m/s)	$\Delta T/\Delta x$ (10^{-6} K/m)	$\Delta u/\Delta x$ (10^{-5} s^{-1})	$\Delta v/\Delta x$ (10^{-5} s^{-1})	$(\Delta u/\Delta x)(\Delta T/\Delta x)$ (10^{-10} K/m/s)
synoptic-scale	FPN	11.5	2.5	9.0	9	−9	7	−8
front	Helgoland	4.0	2.0	2.0	26	−4	2	−11
	Nordholz	3.0	−1.0	4.0	47	3	5	16
sea-breeze	Nordholz	6.0	2.5	3.5	265	−15	22	−408
front	Hamburg	9.7	3.2	6.5	347	−125	90	−4338

Data are taken from Figs. 7, 10 and 13. The cross-frontal distance Δx is estimated according to (2) using a constant frontal speed c_F of 6 m/s. T, u, v and t represent air temperature, cross-frontal wind component, along-frontal wind component and time, respectively.

Table 2. *Frontal propagation speed c_F estimated from time difference Δt_F between frontal passages t_F at two neighbouring stations with cross-frontal distances Δx; the wind speed u_b behind the front is taken from Table 1*

Front	Location	t_F (UT)	Δt_F (min)	Δx (km)	c_F (m/s)	u_b (m/s)
synoptic-scale	FPN	0715				9.0
front			145	74	8.5	
	Helgoland	0940				5.0
			215	60	4.6	
	Nordholz	1315				3.5
sea-breeze	Nordholz	1115				3.5
front			190	74	6.5	
	Hamburg	1425				8.0

latter estimates are listed in Table 2. The synoptic-scale front reduced its speed from 8.5 m/s between FPN and Helgoland to 4.6 m/s between Helgoland and Nordholz. This deceleration is significant because the uncertainty for c_F amounts to about ± 1 m/s if we assume an uncertainty of ± 15 min for the travel time Δt_F. The average propagation speed of the sea-breeze front between Nordholz and Hamburg-Billwerder was 6.5 m/s.

For comparison, the magnitude of the low-level cross-frontal wind component u_b in the cold air behind the front is also listed in Table 2. Taking the average values of u_b between two neighbouring stations, we can conclude that the front changed from a propagating front with $u_b - c_F < 0$ over the sea to a gravity current type front with $u_b - c_F > 0$ over the land. The same changes have been observed by Garatt (1988) for summertime cold fronts approaching the southeast coast of Australia and have been modeled by Physick (1988). If we apply the well-known formula for the propagation speed of a gravity current (e.g., Carbone, 1982; Koch, 1984):

$$c_{\text{grav.curr.}} = k\sqrt{gh\,\Delta\Theta/\Theta}, \tag{7}$$

to the observations at Hamburg-Billwerder and use 400 m for the depth h of the cold air, 2.5 K for the potential temperature difference $\Delta\Theta$ between the warm and the cold air, 292 K as reference potential temperature Θ, 9.81 m/s^2 for the earth's gravity g and 1.1 for the "constant" k, we obtain 6.4 m/s for $c_{\text{grav.curr.}}$. This is very near to the value of 6.5 m/s quoted in Table 2 and is further evidence for the gravity current character of the front over land.

The described interaction between synoptic-scale front and sea-breeze front was only possible because several favourable conditions came together. First, the synoptic-scale front was oriented parallel to the coastline allowing interactions in the same vertical plane between cross-frontal circulations and emerging cross-coastal circulations.

Second, the cloudless conditions ahead of the synoptic-scale front enabled the large differences of solar heating of the land and sea surface and thus the thermal forcing of the sea-breeze circulation.

Third, the nearly coast-parallel geostrophic wind ahead of the synoptic-scale front was favourable for the development of cross-coastal circulations forced by the thermal as well as by the frictional sea-land contrast (e.g., Van de Berg and Oerlemans, 1985; Roeloffzen et al., 1986).

Fourth, the temporal conditions were favourable as far as the time of the day and the spatial distance between synoptic-scale front and sea-breeze front are concerned. Such an interaction would not have taken place during night-time or if the distance between both fronts would have been much wider.

Fifth, convection with clouds extending higher than the top flight level of 3.1 km height developed on the warm-air side of the sea-breeze front. This implies a mesoscale circulation in the vertical plane of similar extent and thus is a depth which is comparable with that at the synoptic-scale front. We suppose that the relatively large vertical and presumably also horizontal extent of the sea-breeze front circulation allowed the connection between both circulation regimes. A much shallower and weaker sea-breeze front circulation would probably not have been able to close this connection and the weak and further weakening circulation at the leading edge of the synoptic-scale front would not have been able to do this anyway.

Sixth, a favourable condition to close the connection between both circulation regimes was probably the existence of a low-level inversion at 200 to 300 m height ahead of the synoptic-scale front over the cool sea (Fig. 12). The cool air below the prefrontal inversion was only little warmer (about 1–2 K) than the low-level air behind the front (Figs. 7, 12). Thus, the low-level branch of the sea-breeze circulation directed from sea to land, had a quasi direct connection to the cold air pool behind the synoptic-scale front via the low-level inversion "channel".

Seventh, the low-level jet with high values of the front-parallel wind component v in the region ahead of the synoptic-scale front (Figs. 8, 11) may have played an important role for the height development of the sea-breeze front and the generation of deep convection on the warm-air side. Low-level jets or zones of increased v wind are an ubiquitous feature of mid-latitude cold fronts (e.g., Browning and Pardoe, 1973). The cyclonic-shear side of the jet ahead of the surface cold front is known to be a region of updraught and intense convection (called "line convection" or "narrow cold-frontal rainband") for which several physical mechanisms can be responsible (Kotroni et al., 1994). At least the wind measurements at Nordholz in Fig. 11 show that the jet maximum had already passed this station and that the sea-breeze front developed on the cyclonic-shear side of the jet axis. However, the quantitative role of the low-level jet for the interaction between the sea-breeze front and the synoptic-scale front cannot be assessed from the available observations and must remain tentatively.

A summary of the observational findings concerning both fronts and of the hypothezised circulation processes is presented schematically in Fig. 15.

In the companion paper Rhodin (1995) presents numerical simulations of a cold front approaching the coast and of an evolving sea-breeze front. The simulations resolve the temporal development of both fronts and their merger. Moreover, the simulations elucidate the main physical processes involved and the dependence of the development on the special conditions met.

As a large number of fronts approach the coastal region of Northern Germany (Hennemuth and Brümmer, 1990) the modifying effect by differential sea-land heating and by coastal circulations may be of climatological importance. Cold fronts

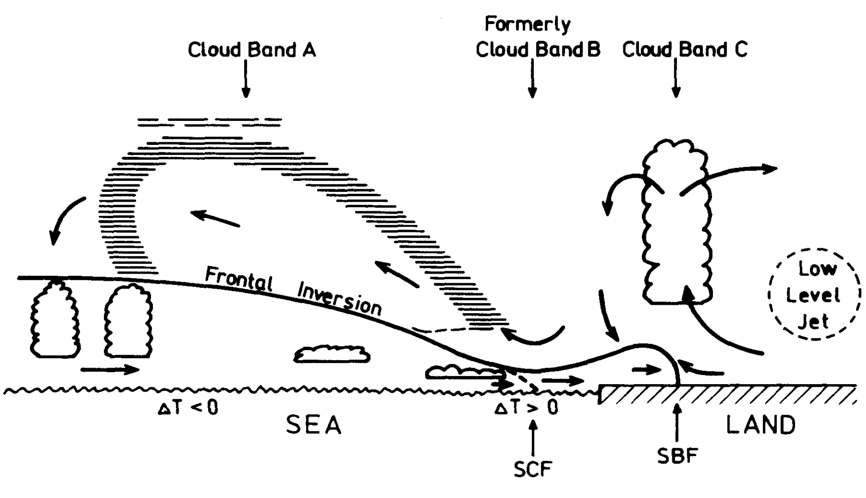

Fig. 15. Summarizing sketch of synoptic-scale front and sea-breeze front and hypothezised interaction processes at a stage when the sea-breeze front is about 20–30 km inland from the coast. "SBF" and "SCF" mark surface positions of sea-breeze front and synoptic-scale front, respectively. ΔT denotes the air-sea temperature difference.

which pass the coastline in the warm season during daytime are expected to be intensified. The presented case study shows that this intensification occurs within a region of several ten kilometers width inland from the coast.

With respect to the thermal effects the prefrontal conditions at the coast can have some similarity to those, when a cold front approaches a mountain barrier and the prefrontal air encounters heating by a prefrontal foehn, as observed during the "German Frontexperiment" in the Alpine foreland (Egger and Hoinka, 1992).

5. Acknowledgements

This study was sponsored by the German Science Foundation. The authors are indebted to M. Lüdicke for preparing the figures and S. Lehmann for typing the manuscript.

REFERENCES

Ball, F. K. 1960. A theory of fronts in relation to surface stress. *Quart. J. R. Met. Soc.* **96**, 51–66.

Bennetts, D. A. and Ryder, P. 1984. A study of mesoscale convective bands behind cold fronts. Part I: Mesoscale organization. *Quart. J. R. Met. Soc.* **110**, 121–145.

Bergeron, T. 1949. The problem of artificial control of rainfall on the globe. Part II: The coastal orographic maxima of precipitation in autumn and winter. *Tellus* **1**, 15–32.

Bond, N. A. and Fleagle, R. G. 1985. Structure of a cold front over the ocean. *Quart. J. R. Met. Soc.* **111**, 739–759.

Bond, N. A. and Shapiro, M. A. 1991. Research aircraft observations of the mesoscale and microscale structure of a cold front over the eastern Pacific Ocean. *Mon. Wea. Rev.* **119**, 3080–3094.

Browning, K. A. and Pardoe, C. W. 1973. Structure of low-level jet streams ahead of mid-latitude cold fronts. *Quart. J. R. Met. Soc.* **99**, 619–638.

Brümmer, B. 1988. Structure and circulation in the boundary layer at a strong cold front. *Contr. Atm. Phys.* **61**, 232–243.

Brümmer, B. (ed.) 1990. FRONTEX 1989, Frontenexperiment im norddeutschen Küstenbereich. Bericht über die Feldmessungen mit einigen Meßbeispielen. *Hamburger Geophys. Einzelschr.* **B7**, 175 pp.

Carbone, R. 1982. A severe frontal rainband. Part I: Stormwide hydrodynamic structure. *J. Atmos. Sci.* **39**, 258–279.

Dunst, M. and Rhodin, A. 1990. On the influence of frictional effects on surface fronts. *Contr. Atm. Phys.* **63**, 223–242.

Egger, J. 1988. Frictionally induced circulations in fronts. *Contr. Atm. Phys.* **61**, 140–142.

Egger, J. and Hoinka, K. P. 1992. Fronts and orography. *Meteorol. Atm. Phys.* **48**, 3–36.

Emmanuel, K. A. 1983. Conditional symmetric instability: a theory for rainbands within extratropical cyclones. In: Lilly and Gal-Chen (eds.): *Mesoscale meteorology, Theories, observations and models.* NATO ASI Series C 114, Dordrecht, 231–245.

Garratt, J. R. 1986. Boundary-layer effects on cold fronts at a coastline. *Bound. Layer Meteorol.* **36**, 101–105.

Garratt, J. R. 1988. Summertime cold fronts in southeast Australia, behaviour and low-level structure of main frontal types. *Mon. Wea. Rev.* **116**, 636–649.

Garratt, J. R., Howells, P. A. C. and Kowalczyk, E. 1989. The behaviour of dry cold fronts traveling along a coastline. *Mon. Wea. Rev.* **117**, 1208–1220.

Hakim, G. J. 1992. The eastern United States side-door front of 22 April 1987: A case study of an intense atmospheric density current. *Mon. Wea. Rev.* **120**, 2738–2762.

Hennemuth, B. and Brümmer, B. 1990. A statistical study of atmospheric fronts in the coastal region of Northern Germany. *Meteorol. Rdsch.* **43**, 1–16.

Hennemuth, B., Thiemann, S., Brümmer, B. and Falke, M. 1991. FRONTEX 1989, Messergebnisse zu neun Kaltfronten. *Ber. Zentr. f. Meeres- und Klimaforsch.*, Univ. Hamburg, nr. **18**, 185 pp.

Hoskins, B. J., Draghici, I. and Davies, H. C. 1978. A new look at the ω-equation. *Quart. J. R. Met. Soc.* **104**, 31–38.

Houze, R. A. and Hobbs, P. V. 1982. Organization and structure of precipitating cloud systems. *Adv. Geophys.* **24**, 225–315.

Keyser, D., Schmidt, B. D. and Duffy, D. G. 1992. Quasigeostrophic vertical motions diagnosed from along- and cross-isentrope components of the Q vector. *Mon. Wea. Rev.* **120**, 731–741.

Koch, S. E. 1984. The role of an apparent mesoscale frontogenetic circulation in squall line initiation. *Mon. Wea. Rev.* **112**, 2090–2111.

Kotroni, V., Lemaitre, Y. and Petitdidier, M. 1994. Dynamics of a low-level jet observed during the Fronts 87 experiment. *Quart. J. R. Met. Soc.* **120**, 277–303.

Kraus, H., Hacker, J. M. and Hartmann, J. 1990. An observational aircraft-based study of sea-breeze frontogenesis. *Bound. Layer Meteorol.* **53**, 223–265.

Kurz, M. 1982. Zum Einfluß diabatischer Prozesse auf die Frontogenese in Bodennähe. *Meteorol. Rdsch.* **35**, 21–30.

Kurz, M. 1992. Synoptic diagnosis of frontogenetic and cyclogenetic processes. *Meteorol. Atmos. Phys.* **48**, 77–91.

Lagouvardos, K., Lemaitre, Y. and Scialom, G. 1992.

Mesoscale ageostrophic circulations of two fronts observed during the Fronts 87 experiment: diagnosis and interpretation. *Meteorol. Atmos. Phys.* **48**, 293–307.

Physick, W. L. 1988. Mesoscale modeling of a cold front and its interaction with a diurnally heated land mass. *J. Atmos. Sci.* **45**, 3169–3187.

Rhodin, A. 1991. Kaltfronten unter dem Einfluß der Reibung in der Grenzschicht und ihre Modifikation bei unterschiedlicher Bodenrauhigkeit und Bodentemperatur, Numerische Simulationen. PhD Thesis, *Ber. Zentr. für Meeres- und Klimaforschung*, Univ. Hamburg, nr. **15**, 125 pp.

Rhodin, A. 1995. Interaction of a cold front with a sea-breeze front: numerical simulations. *Tellus* **47A**, 403–420.

Roeloffzen, J. C., Van den Berg, W. D. and Oerlemans, J. 1986. Frictional convergence at coastlines. *Tellus* **38A**, 397–411.

Shapiro, M. A. 1984. Meteorological tower measurements of a surface cold front. *Mon. Wea. Rev.* **112**, 1634–1639.

Van de Berg, L. and Oerlemans, J. 1985. Simulation of the sea-breeze front with a model of moist convection. *Tellus* **37A**, 30–40.